

Roles of Trp144 and Tyr203 in copper-containing nitrite reductase from *Achromobacter cycloclastes* IAM1013[☆]

Kazuya Yamaguchi, Kazuyoshi Shuta, Shinnichiro Suzuki^{*}

Department of Chemistry, Graduate School of Science, Osaka University, Toyonaka, Osaka 560-0043, Japan

Received 9 August 2005

Available online 19 August 2005

Abstract

The roles of the Trp144 and Tyr203 residues near the type 1 Cu site of *Achromobacter cycloclastes* nitrite reductase (AcNIR) have been examined with mutants of AcNIR. Tyr203 is located on the protein surface near the type 1 Cu site of AcNIR, and Trp144 is between the Tyr203 and the type 1 Cu center in AcNIR. Single mutation of Trp144 or Tyr203 in AcNIR to Leu resulted in decreased rate constants of intermolecular electron transfer from its cognate pseudoazurin (AcPAZ) ($k_{ET} = 1.9 \times 10^5$, 2.2×10^5 , and $7.3 \times 10^5 \text{ M}^{-1} \text{ s}^{-1}$ for W144L, Y203L, and wild-type AcNIR, respectively). The intermolecular electron transfer rate constant of double mutant AcNIR (W144L/Y203L) was the same as those of single mutants ($k_{ET} = 1.9 \times 10^5 \text{ M}^{-1} \text{ s}^{-1}$ for W144L/Y203L). The redox potentials, coordination structures of the type 1 Cu, and the enzyme activities of AcNIR were affected little by the mutation.

© 2005 Elsevier Inc. All rights reserved.

Keywords: Metalloenzyme; Copper protein; Nitrite reductase; Denitrification; Redox; Electron transfer

Copper-containing nitrite reductase (CuNIR), which is key enzyme in the anaerobic respiration system of denitrifying bacteria [1] and catalyzes the reduction of NO_2^- to NO, has two kinds of Cu centers per 37-kDa subunit. Type 1 Cu accepts an electron from an external electron carrier, and type 2 Cu, which accepts an electron from the reduced type 1 Cu site, is the reduction center of NO_2^- . CuNIRs are classified into three groups by spectroscopic properties of type 1 Cu; blue NIRs, green NIRs, and other NIRs [2–4]. The green CuNIRs from *Achromobacter cycloclastes* and *Alcaligenes faecalis* S-6 accept an electron from the cognate pseudoazurin (PAZ), which is a kind of blue copper protein. The interaction of green CuNIRs with the cognate

PAZ involves a strong electrostatic element [5]. In the type 1 Cu site of green CuNIR from *A. cycloclastes* (AcNIR), four amino acid residues (two His, a Cys, and a Met) form a flattened tetrahedron, as shown Fig. 1.

The redox potential of AcNIR is dependent on the coordination geometry of the type 1 Cu [6]. Although the mutant replacing the Met150 ligand of the type 1 Cu with Gln in AcNIR (M150Q) has ~80% the catalytic activity of AcNIR, the spectral features are similar to those of mavericanin and stellacyanin, having symmetrical tetrahedral geometries with the 2His, Cys, and Gln ligands of the type 1 Cu. As the redox potential of M150Q is +113 mV, being negatively shifted compared to that of wild-type AcNIR (+240 mV) at pH 7.0, the intermolecular electron transfer from AcPAZ (+260 mV) to M150Q has not occurred. The type 1 Cu of AcNIR is buried ~7 Å in the enzyme, and there is the hydrophobic patch on the protein surface centered at the type 1 Cu site. The hydrophobic patch is surrounded by many negatively charged residues (Asp89, Glu118, Glu139, Glu197, Glu201, Glu204, and Asp205), which electrostatically interact with the positively charged Lys residues surrounding the hydrophobic patch of the

[☆] Abbreviations: CuNIR, copper-containing nitrite reductase; AxNIR, copper-containing nitrite reductase from *Alcaligenes xylosoxidans* GIFU1051; EPR, electron paramagnetic resonance; AcNIR, copper-containing nitrite reductase from *Achromobacter cycloclastes* IAM1013; PAZ, pseudoazurin; AcPAZ, pseudoazurin from *Achromobacter cycloclastes* IAM1013; NHE, normal hydrogen electrode.

^{*} Corresponding author. Fax: +81 6 6850 5785.

E-mail address: bic@ch.wani.osaka-u.ac.jp (S. Suzuki).

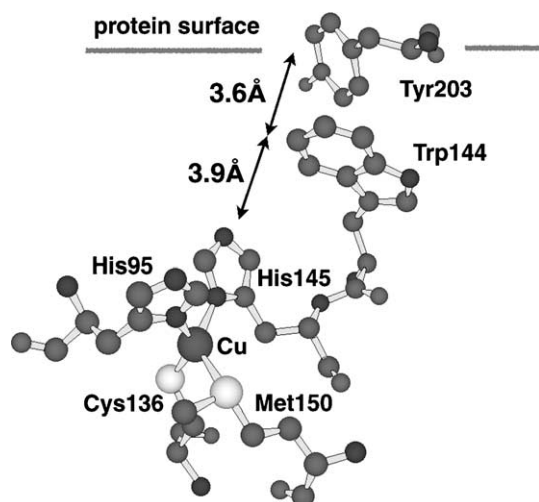


Fig. 1. View of the type 1 Cu site in AcNIR. The type 1 Cu coordinated to the His95, Cys136, His145, and Met150 ligand is buried ~ 7 Å beneath the protein surface. Trp144 is located between Tyr203 on the protein surface and His145.

type 1 Cu site of AcPAZ. The effect of electrostatic interaction between Cu-containing NIR and the electron partner on the intermolecular electron transfer reaction has been studied by using the mutant AxNIRs [5]. It has been found that the intermolecular electron transfer reaction and the formation of an electron transfer complex between AxNIR and AcPAZ are facilitated by the introduction of negatively charged residues in the docking surface of AxNIR.

Tyr203 is situated upon the protein surface near the type 1 Cu of AcNIR. In the docking model of CuNIR and the electron transfer partner, Tyr has been reported to be able to be positioned near the His ligand of type 1 Cu in the partner protein [7,8]. Trp144, which is next to the His145 ligand of the type 1 Cu in AcNIR, is only 3.6 Å apart from the Tyr203.

In order to investigate the roles of Trp144 and Tyr203 in AcNIR for enzymatic activities, spectral features, and intermolecular electron transfer from the electron donor protein, we have replaced these residues of AcNIR with Leu (W144L, Y203L, and W144L/Y203L) by site-directed mutagenesis. In this paper, we report the spectroscopic and electrochemical properties of W144L, Y203L, and W144L/Y203L, and the intermolecular electron transfer reaction between AcNIRs (W144L, Y203L, and W144L/Y203L) and AcPAZ using steady-state kinetics and electrochemical methods. We discuss the effect of Trp144 and Tyr203 of AcNIR for the intermolecular electron transfer with the electron transfer partner protein, AcPAZ.

Materials and methods

Materials. The plasmid vector pMAL-c2X was purchased from New England Biolabs. A *Taq* DNA polymerase, restriction endonucleases, and other modifying enzymes were obtained from Takara Bio and Toyobo. A *Taq* dye-terminator cycle sequencing kit (Applied Biosystems) was used for sequence determination. All other chemicals were of analytical grade. Recombinant AcPAZ and the plasmid pMAcNIR for the expression of

AcNIR as a fusion protein with maltose-binding protein were prepared as reported previously [6,9].

Mutagenesis. Site-directed mutagenesis was performed using the PCR method. For single mutant AcNIRs, we performed a two-step PCR [6], using oligonucleotide primers containing the same mutation (underlined), i.e., 5'-atggtgcccttgacgtcacctcg-3' and 5'-tgacgtgcaagggcaccatgcc-3' (W144L forward and reverse) or 5'-ggcgaagccttagaatgctgtc-3' and 5'-gcattcttaagcttcgccgggg-3' (Y203L forward and reverse) with pMAcNIR as a template. The mutated DNA fragments were digested with restriction enzymes (*Sma*I and *Bam*HI for both W144L and Y203L) and exchanged with the corresponding fragment of pMAcNIR. For the W144L/Y203L double mutant, we carried out the PCR mutagenesis with Y203L forward and reverse oligonucleotide primers and pMAcNIR-W144L as a template. The mutant AcNIR genes (pMAcNIR-W144L, pMAcNIR-Y203L, and pMAcNIR-W144L/Y203L) were sequenced and expressed in *Escherichia coli* JM109 as recombinant proteins. Wild-type and mutant AcNIRs were purified, as described previously [6,9].

Spectral and electrochemical measurements. The electronic absorption spectra of wild-type and mutant AxNIRs were measured at room temperature with a Shimadzu UV-2200 spectrometer. The EPR spectra of frozen protein samples were recorded at 77 K with a JEOL JES-FE1X X-band spectrometer. The concentration of copper was determined with a Nippon Jarrel Ash AA-880 Mark-II atomic absorption spectrophotometer. Cyclic voltammetric analyses were carried out using a Bioanalytical Systems Model CV-50W voltammetric analyzer with a three-electrode system consisting of a Ag/AgCl reference electrode, a gold wire counter electrode, and a bis(4-pyridyl)disulfide-modified gold working electrode under an Ar atmosphere. The intermolecular electron transfer rate constants between PAZ and AcNIR mutants were obtained in 0.1 M phosphate buffer (pH 7.0) at 25.0 °C.

Kinetic analysis. The nitrite reduction activities of mutant AcNIRs were determined by the steady-state method using reduced benzyl viologen as an electron donor [6,9]. The oxidation of reduced benzyl viologen in the presence of the enzyme was spectrophotometrically monitored at 550 nm at 25.0 °C. In order to exclude oxygen gas, the preparation of the reaction mixture was carried out under an argon atmosphere in a glove box. The unit of enzyme activity is defined as the amount of AcNIR that is required to reduce 1 μmol of nitrite per minute.

The kinetic analyses of mutant AcNIRs and AcPAZ were carried out as follows. Reduced AcPAZ was prepared by the addition of 1.2 equiv of ascorbate as a reducing reagent to the solution of the protein, and then the excess reducing reagent was removed by Sephadex G-25 gel filtration under an argon atmosphere in a glove box. The reaction mixture contained 2 mM NaNO₂ and 14–100 μM reduced AcPAZ in a 20 mM potassium phosphate buffer (pH 6.0). The reaction was started by adding appropriate amounts (2.5–10 nM) of mutant AcNIR to the reaction mixture, and the increase in absorbance of oxidized AcPAZ at 593 nm was monitored under anaerobic conditions at 25.0 °C. The molar extinction constant of oxidized AcPAZ ($\epsilon = 3700 \text{ M}^{-1} \text{ cm}^{-1}$ at 593 nm) was used to calculate the kinetic parameters.

Results and discussion

Influence of Trp144 and/or Tyr203 mutation to Leu on the coordination structure of type 1 Cu in AcNIR

Three mutant AcNIRs (W144L, Y203L, and W144L/Y203L) were prepared as described Materials and methods. The molar ratios of the type 1 Cu to the type 2 Cu in the mutants were estimated to be 0.85–0.95 from the atomic absorption spectra of the holo and type 2 copper-depleted mutants. Fig. 2 shows the UV–visible electronic absorption spectra of mutant AcNIRs with those of wild-type AcNIR at pH 7.0. The intensities of absorption band at 280 nm in the mutants were observed to be smaller than

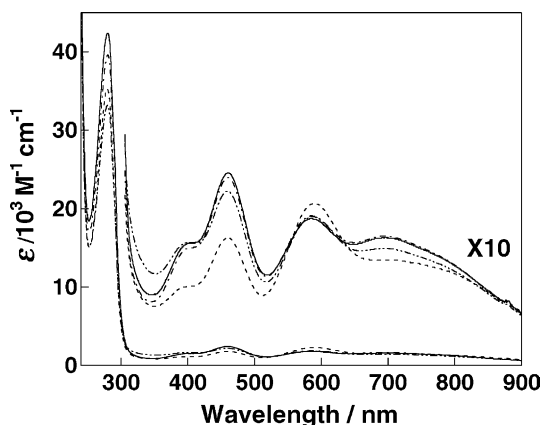


Fig. 2. UV-visible electronic absorption spectra of W144L (broken line), Y203L (dot-dash line), W144L/Y203L (dot-dot-dash line), and wild-type AcNIR (solid line) in 20 mM phosphate buffer (pH 7.0).

that of wild-type AcNIR, because the 280-nm band is due to aromatic amino acid residues such as Trp and Tyr. The visible absorption spectra of wild-type and mutant AcNIRs display three bands at 460, 589, and 690 nm, and a shoulder band around 400 nm, which are characteristic of the type 1 Cu. In wild-type AcNIR having the flattened tetrahedral type 1 Cu center [10,11], two intense bands (460 and 589 nm), a shoulder near 400 nm, and a broad band at 690 nm are assigned to N(His) → Cu, S(Cys) → Cu, and S(Met) → Cu charge transfer transitions and d–d transition of type 1 Cu, respectively [12]. The spectral features of Y203L are almost the same as those of wild-type AcNIR. Although W144L and W144L/Y203L also show the spectra characteristic of the type 1 Cu, the molar extinction coefficients (ϵ) of W144L and W144L/Y203L at 400, 460, and 690 nm are smaller than those of wild-type AcNIR. The absorption spectra of W144L and W144L/Y203L seem to be a compromise of the spectra between green CuNIR (AcNIR) and blue CuNIR (AxNIR), in which the type 1 Cu site is a flattened tetrahedral [10,11] or shows a distorted tetrahedral geometry [13–15], respectively. The results suggest that the mutation of Trp144, which is next to the His145 ligand of the type 1 Cu, influences somewhat the coordination structures of the type 1 Cu site in AcNIR.

The 77-K EPR spectra of wild-type and mutant AcNIRs are shown in Fig. 3. EPR signals of wild-type and mutant AcNIRs displayed the parameters of rhombic type 1 Cu; $g_z = 2.19$, $A_z = 7.3$ mT, $g_y = 2.06$, $g_x = 2.02$, and $A_x = 4.2$ mT, and those of the type 2 Cu; $g_z = 2.33$ and $A_z = 13.0$ mT. The EPR spectra of mutant AcNIRs are different from that of AxNIR, which shows an axial-type EPR spectrum [2]. The EPR spectral data indicate that the coordination structures of the type 1 and 2 Cu sites in all the mutants are quite similar to those in the wild-type AcNIR, and there is little influence of Trp144 and/or Tyr203 mutation to Leu in AcNIR on the electronic structures of the type 1 and 2 copper sites.

The cyclic voltammograms of W144L, Y203L, and W144L/Y203L show well-defined responses with a midpoint

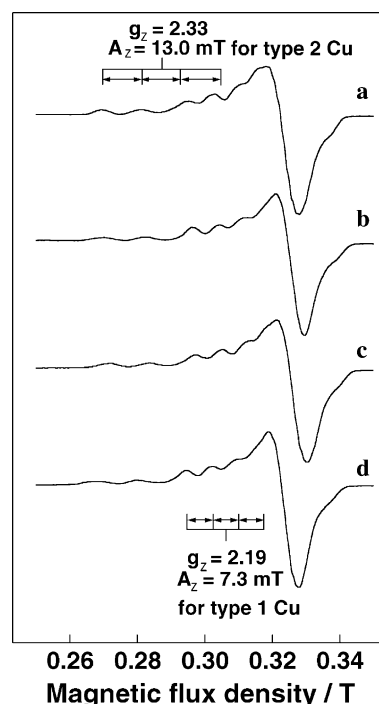


Fig. 3. EPR spectra of (a) wild-type AcNIR, (b) Y203L, (c) W144L, and (d) W144L/Y203L in 20 mM phosphate buffer (pH 7.0) at 77 K.

potential ($E_{1/2}$) of +234, +240, and +241 mV vs. NHE at pH 7.0, respectively. These cyclic voltammetric responses are due to the type 1 Cu in the enzyme, and the $E_{1/2}$ values are almost equal to that of wild-type AcNIR (+240 mV). The redox potential of the type 1 Cu in AcNIR is hardly affected by the mutation of Trp144 and/or Tyr203 to Leu.

Accordingly, these spectral and electrochemical features of mutant AcNIRs suggest that the structure and redox functions of the type 1 Cu in AcNIR are nearly retained in W144L, Y203L, and W144L/Y203L.

Enzyme activities of mutant AcNIRs and the intermolecular electron transfer reactions with AcPAZ

The nitrite reduction activities of mutant AcNIRs were determined by two steady-state methods using either an artificial electron donor (reduced benzyl viologen) or the physiological electron donor (reduced AcPAZ) at pH 6.0 and 25.0 °C. The enzymatic activities ($k_{\text{cat}}^{\text{BV}}$ and $k_{\text{cat}}^{\text{PAZ}}$) are listed in Table 1. The mutants of AcNIR, W144L, Y203L, and W144L/Y203L exhibited almost the same activities ($k_{\text{cat}}^{\text{BV}}$) as the wild-type AcNIR ($2.3 \times 10^3 \text{ s}^{-1}$) with an artificial electron donor. When AcPAZ was used as the electron donor, the activities ($k_{\text{cat}}^{\text{PAZ}}$) of AcNIR mutants were also quite similar to that of wild-type AcNIR (163 s^{-1}) within the range of experimental error. Very recently, Hasnain and his co-investigators [8] have reported that a Trp138His mutant of blue AxNIR had a much reduced activity, ~10% that of the native enzyme, using reduced azurin I as the electron donor. They have suggested that the mutation of Trp138 to His in AxNIR

Table 1

Enzymatic activities ($k_{\text{cat}}^{\text{BV}}$ and $k_{\text{cat}}^{\text{PAZ}}$) of wild-type and mutant AcNIRs, and intermolecular electron transfer rate constants (k_{ET}) between wild-type and mutant AcNIRs and AcPAZ

AcNIRs	$k_{\text{cat}}^{\text{BV}}$ (10^3 s^{-1})	$k_{\text{cat}}^{\text{PAZ}}$ (s^{-1})	k_{ET} ($10^5 \text{ M}^{-1} \text{ s}^{-1}$)
Wild-type	2.3 ± 0.1	163 ± 34	7.3 ± 0.2
W144L	2.1 ± 0.1	140 ± 17	1.9 ± 0.1
Y203L	2.1 ± 0.1	167 ± 23	2.2 ± 0.1
W144L/Y203L	1.9 ± 0.2	180 ± 15	1.9 ± 0.1

has a significant effect on the productive complex formation with azurin I. Our present results that the enzyme activity of AcNIR was little affected by the mutation of Trp144 and/or Tyr203 to Leu in AcNIR indicate that the rate-determining step in the enzyme reaction sequence would not be the formation of a AcNIR–AcPAZ complex, but the reduction of substrate by AcNIR in the steady-state assay system.

The intermolecular electron transfer rate constants (k_{ET}) from AcPAZ to AcNIRs were evaluated by cyclic voltammetry, as reported previously [16]. In the reduction of NO_2^- to NO, the direction of the electron transfer process is as follows: electrode \rightarrow AcPAZ \rightarrow AcNIR \rightarrow NO_2^- . In the electrochemical system, the rate-limiting step is the electron transfer process from AcPAZ to the enzymes, and the rate constant (k_{ET}) is calculated with the following equation [17]:

$$i_{\text{ss}} = nFAC_{\text{PAZ}}(D_{\text{PAZ}}k_{\text{CNIR}})^{0.5},$$

where i_{ss} is the observed catalytic current, C_{PAZ} and C_{NIR} are the solution concentrations of AcPAZ and AcNIR, respectively, D_{PAZ} is the diffusion coefficient of AcPAZ, n is the number of electrons, F is the Faraday constant, and A is the area of the working electrode; k is the homogeneous rate constant for the reaction of reduced AcPAZ with oxidized AcNIR, being equal to the electron transfer rate constant (k_{ET}) from AcPAZ to AcNIR. The k_{ET} from AcPAZ to wild-type AcNIR has previously been reported to be $7.3 \times 10^5 \text{ M}^{-1} \text{ s}^{-1}$ at pH 7.0 [16]. The cyclic voltammograms of (a) AcPAZ, and AcPAZ in the presence of nitrite and (b) wild-type AcNIR, (c) W144L, (d) Y203L or (e) W144L/Y203L at pH 7.0 are shown in Fig. 4. The voltammetric response is affected little by the addition of nitrite to the solution of AcPAZ (a in Fig. 4), suggesting that there is no direct electron transport from the reduced AcPAZ to nitrite. On the addition of AcNIRs to the AcPAZ solution containing nitrite, however, the shape of the voltammogram was dramatically changed and the sigmoidal cathodic current–potential curve (catalytic current) was enhanced (b–e in Fig. 4). The appearance of the catalytic current indicates the regeneration of oxidized AcPAZ by the electron transport from reduced AcPAZ to AcNIR in the diffusion layer. The catalytic current heights of AcNIR mutants (W144L, Y203L, and W144L/Y203L) were smaller than that of wild-type AcNIR. The k_{ET} values calculated with the above equation are listed in Table 1. The single replacement of Trp144 or Tyr203 of AcNIR with non-aro-

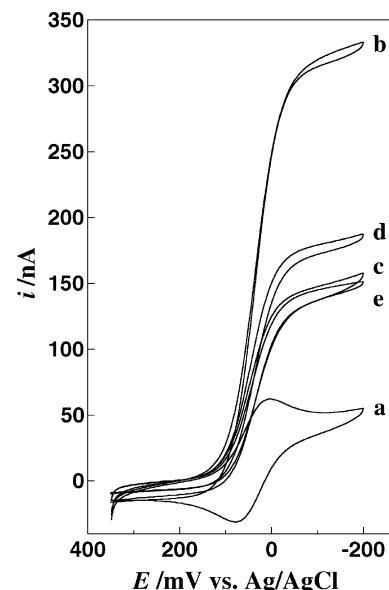


Fig. 4. Voltammetric behavior of (a) AcPAZ, after addition of nitrite and (b) wild-type AcNIR, (c) W144L, (d) Y203L or (e) W144L/Y203L in 100 mM potassium phosphate buffer (pH 7.0) at 25.0 °C. Reaction conditions: AcPAZ, 100 μM ; CuNIRs, 1 μM ; sodium nitrite, 50 mM; scan rate, 2 mV/s.

matic residue (Leu) brings about a 3.6-fold decrease in k_{ET} values (1.9×10^5 and $2.2 \times 10^5 \text{ M}^{-1} \text{ s}^{-1}$, respectively), while the double mutation of Trp144 and Tyr203 of AcNIR to Leu does not cause an additional decrease in k_{ET} values ($1.9 \times 10^5 \text{ M}^{-1} \text{ s}^{-1}$). The π -electron systems of aromatic side chains of Tyr and Trp have been reported to play important roles in electron transfers in some biological systems [18–24], such as intramolecular long-range electron transfer between Tyr and Trp in lysozymes [24]. In the mechanism for electron transfer within and between proteins, electron tunneling along chains between redox centers has been reported to be important essentially [25,26]. A free electron localized on a redox center has a wavefunction decaying exponentially into the electrically insulating amino acid medium. The electron tunneling distance should be 14 Å or less. As the distance between type 1 Cu in AcNIR and the type 1 Cu in AcPAZ is about 13 Å in the docking model of CuNIR and the electron transfer partner [7,8], electron could mainly travel between the type 1 Cu atoms through the protein medium. The intermolecular electron transfer reaction rates between AcNIR and AcPAZ were affected obviously by the mutation of Trp144 and/or Tyr203 in AcNIR. The results suggest that Trp144 and Tyr203 would play a role in constructing a tunneling conduction pathway rather than simply occupying the space between the type 1 Cu atoms.

Conclusions

W144L, Y203L, and W144L/Y203L mutants of AcNIR show visible absorption and EPR spectra similar to those of wild-type AcNIR. The redox potentials of the mutants

are also nearly equal to that of wild-type. These spectral and electrochemical data of mutants suggest that the geometry of the type 1 Cu in AcNIR is little affected by the mutation of Trp144 and/or Tyr203 to Leu. Although the enzymatic activities of the mutants are also the same as that of wild-type enzyme, the intermolecular electron transfer rate constants from AcPAZ to mutant AcNIRs are found to be 3- to 4-fold less than that from AcPAZ to wild-type AcNIR using electrochemical methods. The results imply that the rate-determining step in the enzyme reaction sequence is not the intermolecular electron transfer process between AcPAZ and AcNIR, but the reduction of substrate by AcNIR in the steady-state assay system. Furthermore, the Trp144 and Tyr203 would be suggested to play a role as electron tunneling chain elements in intermolecular electron transfer between AcPAZ and AcNIR.

Acknowledgments

This work was supported by Grant-in-Aid for Scientific Research on Priority Areas (No. 17036037 “Chemistry of Coordination Space,” to K.Y.) from Ministry of Education, Science, Sports and Culture, Japan, and the Center of Excellence (21COE) Program “Creation of Integrated EcoChemistry” of Osaka University.

References

- [1] W.G. Zumft, Cell biology and molecular basis of denitrification, *Microbiol. Mol. Biol. Rev.* 61 (1997) 533–616.
- [2] S. Suzuki, K. Kataoka, K. Yamaguchi, T. Inoue, Y. Kai, Structure–function relationships of copper-containing nitrite reductases, *Coord. Chem. Rev.* 190–192 (1999) 245–265.
- [3] S. Suzuki, K. Kataoka, K. Yamaguchi, Metal coordination and mechanism of multicopper nitrite reductase, *Acc. Chem. Res.* 33 (2000) 728–735.
- [4] K. Yamaguchi, K. Kataoka, M. Kobayashi, K. Itoh, A. Fukui, S. Suzuki, Characterization of two type 1 Cu sites of *Hyphomicrobium denitrificans* nitrite reductase: a new class of copper-containing nitrite reductases, *Biochemistry* 43 (2004) 14180–14188.
- [5] K. Kataoka, K. Yamaguchi, M. Kobayashi, T. Mori, N. Bokui, S. Suzuki, Structure-based engineering of *Alcaligenes xylosoxidans* copper-containing nitrite reductase enhances intermolecular electron transfer reaction with pseudoazurin, *J. Biol. Chem.* 279 (2004) 53374–53378.
- [6] K. Kataoka, K. Yamaguchi, S. Sakai, K. Takagi, S. Suzuki, Characterization and function of Met150Gln mutant of copper-containing nitrite reductase from *Achromobacter cycloclastes* IAM1013, *Biochem. Biophys. Res. Commun.* 303 (2003) 519–524.
- [7] L.M. Murphy, F.E. Dodd, F.K. Yousafzai, R.R. Eady, S.S. Hasnain, Electron donation between copper containing nitrite reductases and cupredoxins: the nature of protein–protein interaction in complex formation, *J. Mol. Biol.* 315 (2002) 859–871.
- [8] M.L. Barrett, R.L. Harris, S. Antonyuk, M.A. Hough, M.J. Ellis, G. Sawers, R.R. Eady, S.S. Hasnain, Insights into redox partner interactions and substrate binding in nitrite reductase from *Alcaligenes xylosoxidans*: crystal structures of the Trp138His and His313Gln mutants, *Biochemistry* 43 (2004) 16311–16319.
- [9] K. Kataoka, H. Furusawa, K. Takagi, K. Yamaguchi, S. Suzuki, Functional analysis of conserved aspartate and histidine residues located around the type 2 copper site of copper-containing nitrite reductase, *J. Biochem.* 127 (2000) 345–350.
- [10] E.T. Adman, J.W. Godden, S. Turley, The structure of copper-nitrite reductase from *Achromobacter cycloclastes* at five pH values, with NO_2^- bound and with type II copper depleted, *J. Biol. Chem.* 270 (1995) 27458–27474.
- [11] M.E.P. Murphy, S. Yurley, E.T. Adman, Structure of nitrite bound to copper-containing nitrite reductase from *Alcaligenes faecalis*, *J. Biol. Chem.* 272 (1997) 28455–28460.
- [12] L.B. LaCroix, S.E. Shadle, Y. Wang, B.A. Averill, B. Hedman, K.O. Hodgson, E.I. Solomon, Electronic structure of the perturbed blue copper site in nitrite reductase: spectroscopic properties, bonding, and implications for the entatic/rack state, *J. Am. Chem. Soc.* 118 (1996) 7755–7768.
- [13] F.E. Dodd, S.S. Hasnain, Z.H.L. Abraham, R.R. Eady, B.E. Smith, Structures of a blue-copper nitrite reductase and its substrate-bound complex, *Acta Crystallogr. D* 53 (1997) 406–418.
- [14] F.E. Dodd, J. Van Beeumen, R.R. Eady, S.S. Hasnain, X-ray structure of a blue-copper nitrite reductase in two crystal forms. The nature of the copper sites, mode of substrate binding and recognition by redox partner, *J. Mol. Biol.* 282 (1998) 369–382.
- [15] T. Inoue, M. Gotoda, Deligeer, K. Kataoka, S. Suzuki, K. Yamaguchi, H. Watanabe, M. Goho, Y. Kai, Type 1 Cu structure of blue nitrite reductase from *Alcaligenes xylosoxidans* GIFU 1051 at 2.05 Å resolution: a comparison between blue and green nitrite reductases, *J. Biochem.* 124 (1998) 876–879.
- [16] T. Kohzuma, S. Takase, S. Shidara, S. Suzuki, Electrochemical properties of copper proteins, pseudoazurin, and nitrite reductase from *Achromobacter cycloclastes* IAM 1013, *Chem. Lett.* (1993) 149–152.
- [17] R.S. Nicholson, I. Shain, Theory of stationary electrode polarography, single scan and cyclic methods applied to reversible, irreversible, and kinetic systems, *Anal. Chem.* 36 (1964) 706–723.
- [18] W.A. Prütz, J. Butler, E.J. Land, A.J. Swallow, Direct demonstration of electron transfer between tryptophan and tyrosine in proteins, *Biochem. Biophys. Res. Commun.* 96 (1980) 408–414.
- [19] J. Butler, E.J. Land, W.A. Prütz, A.J. Swallow, Charge transfer between tryptophan and tyrosine in protein, *Biochim. Biophys. Acta* 705 (1982) 150–162.
- [20] M. Faraggi, M.R. DeFelippis, M.H. Klapper, Long-range electron transfer between tyrosine and tryptophan in peptides, *J. Am. Chem. Soc.* 111 (1989) 5141–5145.
- [21] C.-Y. Lee, A possible biological role of the electron transfer between tyrosine and tryptophan, *FEBS Lett.* 299 (1992) 119–123.
- [22] C. Aubert, P. Mathis, A.P.M. Eker, K. Brettel, Intraprotein electron transfer between tyrosine and tryptophan in DNA photolyase from *Anacystis nidulans*, *Proc. Natl. Acad. Sci. USA* 96 (1999) 5423–5427.
- [23] X.-Y. Li, Electron transfer between tryptophan and tyrosine: theoretical calculation of electron transfer matrix element for intramolecular hole transfer, *J. Comp. Chem.* 22 (2001) 565–579.
- [24] M. Stuart-Audette, Y. Blouquit, M. Faraggi, C. Sicard-Roselli, C. Houee-Levin, P. Jolles, Re-evaluation of intramolecular long-range electron transfer between tyrosine and tryptophan in lysozymes: evidence for the participation of other residues, *Eur. J. Biochem.* 270 (2003) 3565–3571.
- [25] C.C. Page, C.C. Moser, X. Chen, P.L. Dutton, Natural engineering principles of electron tunneling in biological oxidation–reduction, *Nature* 402 (1999) 47–52.
- [26] C.C. Page, C.C. Moser, P.L. Dutton, Mechanism for electron transfer within and between proteins, *Curr. Opin. Chem. Biol.* 7 (2003) 551–556.